

Late-stage magmatic outgassing from a volatile-depleted Moon

James M. D. Day, Frédéric Moynier, Charles K. Shearer

► **To cite this version:**

James M. D. Day, Frédéric Moynier, Charles K. Shearer. Late-stage magmatic outgassing from a volatile-depleted Moon. Proceedings of the National Academy of Sciences of the United States of America , National Academy of Sciences, 2017, 114 (36), pp.9547-9551. 10.1073/pnas.1708236114 . insu-02917390

HAL Id: insu-02917390

<https://hal-insu.archives-ouvertes.fr/insu-02917390>

Submitted on 22 Apr 2021

HAL is a multi-disciplinary open access archive for the deposit and dissemination of scientific research documents, whether they are published or not. The documents may come from teaching and research institutions in France or abroad, or from public or private research centers.

L'archive ouverte pluridisciplinaire **HAL**, est destinée au dépôt et à la diffusion de documents scientifiques de niveau recherche, publiés ou non, émanant des établissements d'enseignement et de recherche français ou étrangers, des laboratoires publics ou privés.



Late-stage magmatic outgassing from a volatile-depleted Moon

James M. D. Day^{a,b,1}, Frédéric Moynier^{b,c}, and Charles K. Shearer^d

^aScripps Institution of Oceanography, University of California, San Diego, La Jolla, CA 92093-0244; ^bInstitut de Physique du Globe de Paris, Université Paris Diderot, Sorbonne Paris Cité, 75005 Paris, France; ^cInstitut Universitaire de France, 75005 Paris, France; and ^dInstitute of Meteoritics, University of New Mexico, Albuquerque, NM 87131

Edited by Mark H. Thiemens, University of California, San Diego, La Jolla, CA, and approved July 14, 2017 (received for review May 18, 2017)

The abundance of volatile elements and compounds, such as zinc, potassium, chlorine, and water, provide key evidence for how Earth and the Moon formed and evolved. Currently, evidence exists for a Moon depleted in volatile elements, as well as reservoirs within the Moon with volatile abundances like Earth's depleted upper mantle. Volatile depletion is consistent with catastrophic formation, such as a giant impact, whereas a Moon with Earth-like volatile abundances suggests preservation of these volatiles, or addition through late accretion. We show, using the "Rusty Rock" impact melt breccia, 66095, that volatile enrichment on the lunar surface occurred through vapor condensation. Isotopically light Zn ($\delta^{66}\text{Zn} = -13.7\%$), heavy Cl ($\delta^{37}\text{Cl} = +15\%$), and high U/Pb supports the origin of condensates from a volatile-poor internal source formed during thermomagmatic evolution of the Moon, with long-term depletion in incompatible Cl and Pb, and lesser depletion of more-compatible Zn. Leaching experiments on mare basalt 14053 demonstrate that isotopically light Zn condensates also occur on some mare basalts after their crystallization, confirming a volatile-depleted lunar interior source with homogeneous $\delta^{66}\text{Zn} \approx +1.4\%$. Our results show that much of the lunar interior must be significantly depleted in volatile elements and compounds and that volatile-rich rocks on the lunar surface formed through vapor condensation. Volatiles detected by remote sensing on the surface of the Moon likely have a partially condensate origin from its interior.

Moon | volatile-poor | Rusty Rock | magma ocean | condensates

Extreme depletions of volatile elements in lunar rocks, compared with primitive meteorites and Earth, have been used as evidence of catastrophic degassing of the material that formed the Moon (1, 2). Stable isotope signatures of Zn (3, 4), K (5), and Cl (6) have been used to demonstrate depletion in these elements through evaporative loss during and/or following the formation of the Moon. Variable Cl and Zn isotopic compositions for lunar rocks have been interpreted to reflect local eruptive degassing (6), or lunar magma ocean outgassing (1, 4, 7). Conversely, relative homogeneity of Zn isotopes in mare basalts is consistent with volatile depletion during a Moon-forming giant impact (3). A volatile-depleted Moon supports a highly energetic formation process, where the proto-Earth and another planetary body collided (8, 9), leading to partial to complete melting of their silicate mantles (10).

Not all evidence points to a volatile-depleted Moon. Lunar crustal rocks relatively enriched in moderately volatile elements have been documented since the Apollo missions (11). Lunar volcanic glass bead deposits have lower $^{206}\text{Pb}/^{204}\text{Pb}$ than mare basalts, implying a source with $^{238}\text{U}/^{204}\text{Pb}$ as low as ~ 25 ; only some four times more depleted in the moderately volatile element Pb than in Earth's mantle [$^{238}\text{U}/^{204}\text{Pb} = \sim 6$ to 8 (12)]. Olivine-hosted melt inclusions from the high-Ti lunar volcanic glass, 74220, contain elevated abundances of OH, F, Cl, and S, implying a lunar interior with volatile contents like Earth's depleted upper mantle (13), with several mare basalt melt inclusions showing similar F, Cl, and S enrichments (14). Some mare basalt apatite grains have a substantial OH component (15), and anomalously isotopically light Zn compositions characterize the

volcanic glasses and some mare basalts, such as 14053 (4, 16, 17). These signatures are inconsistent with complete evaporative loss of volatile elements from the Moon, requiring that volatile components exist within and on the Moon. The origin of these volatiles, however, remains enigmatic. These observations challenge notions of a completely "dry" Moon, suggesting that the lunar volatile element inventory might even approach levels like that in Earth.

Lunar "Rusty Rock"

The Rusty Rock, 66095, is an example of a volatile-enriched lunar sample, with elevated contents of Bi, Br, Cd, Cl, Ge, In, Pb, Sb, Tl, and Zn compared with other lunar samples (11, 18–20). It is an impact melt breccia containing clasts of anorthosite, troctolite, and basalt and an incompatible-element-rich (potassium, rare earth element, phosphorous-rich, or "KREEPY") geochemical signature. Fragments of the impact melt breccia define an ^{87}Rb – ^{87}Sr formation age of 4.06 ± 0.24 Ga (*SI Appendix*) that is identical, within uncertainty, to the ^{207}Pb – ^{206}Pb age of 4.01 ± 0.06 Ga (21). Initial $^{87}\text{Sr}/^{86}\text{Sr}$ for 66095 is 0.69909 ± 5 , consistent with a source with low long-term time-integrated Rb/Sr, and that demonstrates a lunar origin. Eighty-five percent of Pb in 66095 is unsupported by radioactive decay of U and Th, requiring a source for the Pb with high U [$^{238}\text{U}/^{204}\text{Pb} = >570$ (21)], again, indicating a lunar origin for Pb within the sample. The rusty character of 66095 is due to the presence of akagenite [FeOOH (22)] and lawrencite [FeCl₂ (23)], leading to the hypothesis that volatile element enrichment occurred in 66095 through fumarolic activity (11, 21, 23).

To investigate the origin of volatile enrichment in lunar rocks, we analyzed three separate fragments of 66095, two dominated by impact melt breccia [66095, 421 and 430] and one of cataclastic

Significance

The "Rusty Rock" 66095 is one of the most volatile-rich rocks from the Moon. The abundance and isotopic composition of volatile elements in the Rusty Rock demonstrates that its lunar interior source became highly depleted in volatile elements and compounds, including Zn, Cl, and Pb. Depletion of these and other volatile elements occurred during thermomagmatic evolution of the Moon and a magma ocean phase. The volatile-rich nature of some rocks on the lunar surface likely originates from extreme degassing and volatile loss from the Moon's interior. Light zinc isotopic compositions in the Rusty Rock and in the lunar volcanic glass beads (74220, 15426) imply that these samples are partly derived from reservoirs that experienced vapor condensation from a volatile-poor Moon.

Author contributions: J.M.D.D. designed research; J.M.D.D., F.M., and C.K.S. performed research; J.M.D.D., F.M., and C.K.S. contributed new reagents/analytic tools; J.M.D.D., F.M., and C.K.S. analyzed data; and J.M.D.D. wrote the paper.

The authors declare no conflict of interest.

This article is a PNAS Direct Submission.

¹To whom correspondence should be addressed. Email: jmdday@ucsd.edu.

This article contains supporting information online at www.pnas.org/lookup/suppl/doi:10.1073/pnas.1708236114/-DCSupplemental.

anorthosite with glass [66095, 425] that has low rare earth element abundances, a large positive Eu anomaly, and a radiogenic initial $^{87}\text{Sr}/^{86}\text{Sr}$ ratio. The highly siderophile element (HSE) abundances in the studied fragments of 66095 are between 0.001 and $0.02 \times \text{CI}$ chondrite, corresponding to ~ 0.3 to 1.3% by mass of impactor contamination. The Re–Os isotope system is disturbed, with fragments having subchondritic to slightly superchondritic measured $^{187}\text{Os}/^{188}\text{Os}$ (0.1226 to 0.1367). Zinc is located within sphalerite (ZnS) grains that are associated with troilite (FeS) (*SI Appendix*). Chlorine is more heterogeneously distributed, altering metal grains and leading to formation of lawrencite (23). Zinc and Cl abundances are correlated in fragments of 66095 (18), consistent with the generation of sphalerite and lawrencite by the reaction: $\text{ZnCl}_2(\text{g}) + \text{FeS}(\text{s}) \leftrightarrow \text{ZnS}(\text{s}) + \text{FeCl}_2(\text{s})$, constrained by ZnS–FeS–Fe equilibrium at between 200 °C and 600 °C (*SI Appendix*). While, in detail, these are not the only reactions, such conditions indicate vapor deposition or condensation by localized fumerolic activity on the lunar surface at or during the time of formation of sample 66095. The variable Fe/Zn ratios for fractions of the sample (1.2 to 357) are consistent with a nonmagmatic origin for the Zn. We also analyzed leachates of the Apollo mare basalt 14053, to search for isotopically light condensates that might explain its bulk isotopic composition (4).

Zinc isotope compositions {expressed as $\delta^X\text{Zn} = [({}^X\text{Zn}/{}^{64}\text{Zn})_{\text{sample}} / ({}^X\text{Zn}/{}^{64}\text{Zn})_{\text{JMC-Lyon}} - 1] \times 1,000$, where $X\text{Zn}$ equals either ${}^{66}\text{Zn}$, ${}^{67}\text{Zn}$, or ${}^{68}\text{Zn}$ } were measured in bulk rocks and in leaches and residues of 66095, and from 14053. Leaching was performed to assess homogeneity of Zn isotopes within 66095 and to investigate if isotopically light Zn measured previously in five mare basalts (10017, 12005, 12018, 14053, and 15016) could be an inherent feature, or result from isotopically light condensates added after the rocks had crystallized (3, 4). Bulk-rock, residue, and leachate data for 66095 span a range of $\delta^{66}\text{Zn}$ from -8.1 to -14‰ , defining kinetic isotopic fractionation lines corresponding to slopes of ~ 1.5 and ~ 2 , respectively, for $\delta^{67}\text{Zn}$ ($1.5022 \times \delta^{66}\text{Zn}$; $R^2 = >0.99$) and $\delta^{68}\text{Zn}$ ($2.0037 \times \delta^{66}\text{Zn}$; $R^2 = >0.99$) (Fig. 1). The results demonstrate mass-dependent behavior of Zn isotopes within 66095 and indicate that the entire inventory of Zn is isotopically light, and distinct from possible impactor materials (3). The results are also distinct from the effect of impact gardening on the lunar surface by small impacts

(16, 17). Residue, hydrochloric acid, and water leaches of 14053 all gave isotopically light Zn values [$\delta^{66}\text{Zn}$ of -1.3 to -0.1‰], whereas the hydrofluoric–nitric acid leach, which was designed to attack silicates, gave a value of $\delta^{66}\text{Zn}$ of $+1.6\text{‰}$, with $0.6 \mu\text{g}\cdot\text{g}^{-1}$ Zn.

The bulk rock of 66095 (-13.7‰) has the most negative $\delta^{66}\text{Zn}$ value measured to date from the Moon. The abundance of Zn in bulk-rock fragments ($100 \mu\text{g}\cdot\text{g}^{-1}$ to $400 \mu\text{g}\cdot\text{g}^{-1}$) is 70 to 300 times greater than the median Zn abundance in mare basalts ($1.3 \mu\text{g}\cdot\text{g}^{-1}$). Fractionation between vapor and melt (α) in a vacuum during Rayleigh distillation $\{\delta_{\text{final}} = \delta_{\text{initial}} + [(1,000 + \delta_{\text{initial}}) (F^{(\alpha-1)} - 1)]\}$, where F is the fraction of Zn remaining in the melt} can be approximated as the square root of the light isotopolog over the heavy isotopolog of the vaporizing species. For ZnCl_2 , the α value ranges from 0.993 (${}^{64}\text{Zn}^{37}\text{Cl}_2/{}^{66}\text{Zn}^{37}\text{Cl}_2$) to as low as 0.978 (${}^{64}\text{Zn}^{35}\text{Cl}_2/{}^{66}\text{Zn}^{37}\text{Cl}_2$). Conversely to Zn, the Cl isotope composition of the Rusty Rock is isotopically heavy [$\delta^{37}\text{Cl} = +15\text{‰}$ (23)], suggesting a different sense of isotopic fractionation. Maximum Zn isotopic fractionation occurs at the lowest and highest extents of fractional volatile loss, leading, at the lowest extents of vapor loss, to a value of $\delta^{66}\text{Zn}$ of $\sim -7\text{‰}$, assuming a starting composition of 0‰ and $\alpha = 0.993$. To arrive at a value of -13.7‰ , at least one further phase of evaporation and condensation is required, or a lower α factor would have to be imparted (~ 0.985), contrasting with the subdued bulk α factor determined in analogs (24). Conversely, the $\delta^{37}\text{Cl}$ of the Rusty Rock requires vapor condensates from a highly depleted source that was already depleted in bulk Cl and enriched in ^{37}Cl .

Volatile-Poor Lunar Source

Isotopically light Zn, heavy Cl (23), and high $^{206}\text{Pb}/^{204}\text{Pb}$ (21) in 66095 cannot be collectively reconciled by a single phase of evaporation at the lunar surface. Impactor material within 66095 has a broadly chondritic HSE composition, yet no chondrites or other potential impactor materials have the combination of Cl–Zn–Pb isotope and HSE characteristics like those observed in 66095 (3, 25). Melt breccia formation ages for 66095, from Rb–Sr and U–Pb isotope systematics, indicate that fumerolic activity probably occurred at the same time—or slightly after—the impact processes responsible for forming the rock, with the Pb content controlled by sulfide. Impact melt rocks can have heavier $\delta^{37}\text{Cl}$ than mare basalts (7), and 66095 has high $\delta^{37}\text{Cl}$, low initial Rb/Sr, and radiogenic $^{206}\text{Pb}/^{204}\text{Pb}$. The Pb implies long-term development in a high- μ source [$^{238}\text{U}/^{204}\text{Pb} = \sim 800$ at 4.5 Ga], and, with the low Rb/Sr and low Cl content implied from heavy $\delta^{37}\text{Cl}$, can only be reconciled through vapor condensation from an ancient, volatile-poor lunar interior source, not from possible volatile-rich sources involved in the formation of the impact melt breccia. Conversely, the Zn isotope composition of 66095 requires a lunar source relatively rich in Zn, compared with Cl.

A distinction between Cl, Zn, and Pb is that they have different partitioning behavior during magmatic crystallization. Zinc is a moderately compatible element during silicate crystallization, with olivine melt partitioning of ~ 1 (26), whereas both Cl and Pb are highly incompatible until crystallization of apatite and plagioclase/sulfides, respectively (15, 27). In a lunar magma ocean, mafic silicate phases crystallized early, whereas plagioclase is not predicted to have formed until $\sim 80\%$ crystallization, with apatite and sulfides forming late in the crystallization sequence (28). While all three of these moderately volatile elements can be lost from the lunar surface by evaporation (1), Zn will be retained within early crystallizing phases, whereas Cl and Pb will not be retained until late-stage crystallization in a magma ocean (Fig. 2). Since the precursor lithology to 66095 is expected to have formed from magma ocean processes, it would be strongly depleted in Pb and Cl. In turn, an isotopically heavy Cl signature and high U/Pb would be predicted due to near-complete loss of Cl and Pb during evaporation from a magma ocean. In contrast, less Zn would be lost due to retention in

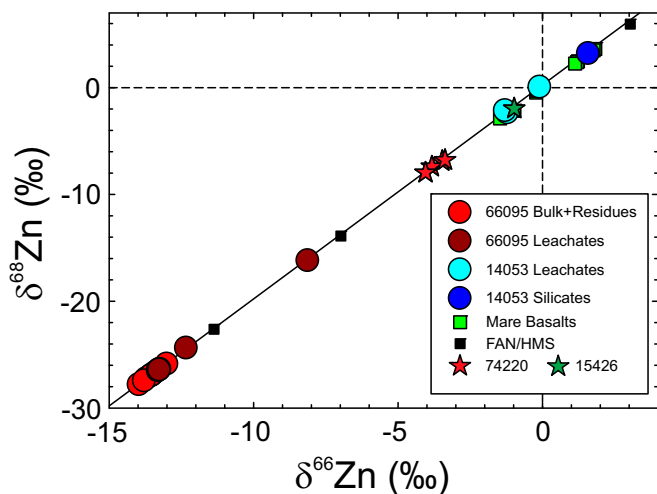


Fig. 1. Values of $\delta^{68}\text{Zn}$ versus $\delta^{66}\text{Zn}$ for components in Apollo 66095 and 14053, and for previously published mare basalt, FAN, high-Mg suite (HMS), and lunar volcanic beads, 74220 and 15426 (3, 4). Dashed lines denote zero values, and solid line denotes regression through 66095 and 14053 data, collected during the same analytical campaign (slope of 2.0037; $R^2 = 0.9999$).

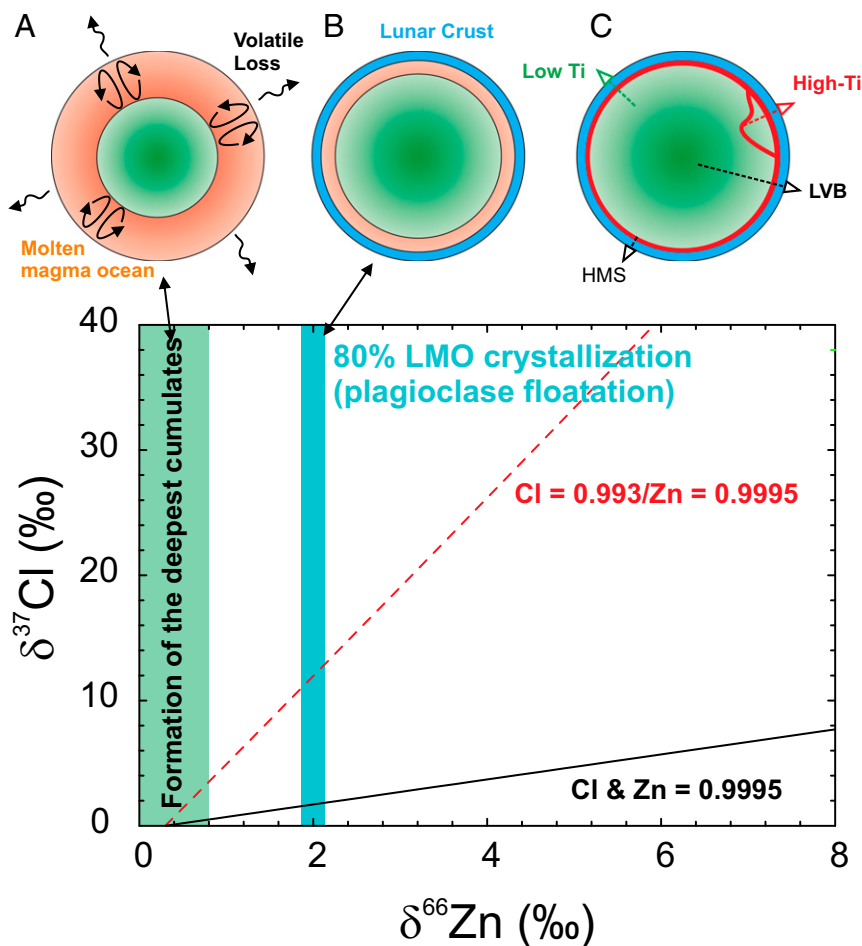


Fig. 2. Chlorine versus Zn isotopic evolution in a progressively crystallizing magma ocean at different fractionation factors for Cl ($\alpha = 0.9995$ to 0.993). Preferential retention of Zn due to olivine melt partitioning of ~ 1 , compared with < 1 for Cl (and Pb) leads to rapid depletion in Pb and Cl in the Moon, even with an α fractionation of 0.9995 . The isotopically heavy Cl, high U/Pb, and moderately positive $\delta^{66}\text{Zn}$ therefore reflects different preservation of moderately volatile elements in a crystallizing Moon. Volatile loss would commence with the earliest and most volatile-rich magma ocean cumulates (stage a), to crust formation (stage b), followed by late-stage intrusion, Fe–Ti oxide overturn, and mare basalt magmatism (stage c). The starting composition for lunar evolution is assumed to be identical to that of the bulk silicate Earth in this model ($\delta^{37}\text{Cl} = \sim 0\text{‰}$; $\delta^{66}\text{Zn} = \sim 0.3\text{‰}$). High-Ti, high-Ti mare basalts; HMS, high-Mg suite; Low Ti, low-Ti mare basalts; LVB, lunar volcanic beads.

crystallizing silicate phases. Rusty Rock 66095 therefore experienced fumerolic activity that condensed vapor originating from endogenous source rocks that were already significantly volatile-depleted. Given that the clast population of 66095 is dominated by anorthosite, and the initial $^{87}\text{Sr}/^{86}\text{Sr}$ of the impact melt breccia suggests a source with low Rb/Sr like ferroan anorthositic (FAN), it strongly implies that the volatile element isotopic character of 66095 was inherited from the lunar crust.

Condensates on the Moon's Surface

Recognition of evaporative loss of Zn, Cl, and Pb both before and during fumerolic activity from impact processes on the surface of the Moon has wide-ranging implications. First, the presence of isotopically light Zn in 66095 unequivocally demonstrates that condensates of Zn and other volatile elements occur on the lunar surface, providing compelling evidence that remotely sensed volatile-rich deposits on the Moon may have a partly endogenous origin (29). Condensate Zn, after evaporative fractionation, has been suggested as an explanation for isotopically light Zn values measured in some mare basalts (3). The leaching experiments of the mare basalt 14053 ratify this suggestion, with silicates having heavy $\delta^{66}\text{Zn}$ ($+1.6\text{‰}$), and a low Zn concentration ($0.6 \mu\text{g}\cdot\text{g}^{-1}$), compared with the bulk-rock composition [$\delta^{66}\text{Zn} = -1\text{‰}$; $\text{Zn} = 2.7 \mu\text{g}\cdot\text{g}^{-1}$ (4)]. We can confirm an isotopically heavy lunar Zn

composition for the mare basalt sources of $\sim +1.4 \pm 0.5\text{‰}$ (4) determined from samples with low Zn abundances and no evidence for condensate Zn contamination (Fig. 3).

Ancient surface rocks of the lunar crust, including FANs, became enriched in Zn through vapor condensation. FANs have Zn abundances ($0.6 \mu\text{g}\cdot\text{g}^{-1}$ to $75 \mu\text{g}\cdot\text{g}^{-1}$) and $\delta^{66}\text{Zn}$ [$+4.2$ to -11.4‰ (4)] that correlate negatively. Given the high Zn content and isotopically light Zn value for 66095, it is possible to ascertain that the lowest Zn abundance FAN (15415) is the least affected by vapor condensation of Zn like that found in 66095. A minimum estimate for the $\delta^{66}\text{Zn}$ value of FAN is $+4.2\text{‰}$, similar to the values measured in lunar crustal HMS and alkali suite rocks [$+3$ to $+6.3\text{‰}$ (4)]. Heterogeneous distribution of Zn in lunar crustal rocks relative to mare basalt sources cannot be reconciled by models of volatile loss during giant impact, because it would lead to a homogeneous $\delta^{66}\text{Zn}$ signature for the Moon. Instead, lunar crustal rocks require partial evaporative loss during a magma ocean phase to explain the progressive enrichment in the heavy isotopes of Zn for the late-formed lunar crust relative to mare basalt sources, followed by vapor condensation and deposition into the lunar crust (Fig. 3). A prediction, therefore, is that Zn, Cl, and K isotopes should all be isotopically heavier in late-stage pristine crustal rocks than in mare basalt sources.

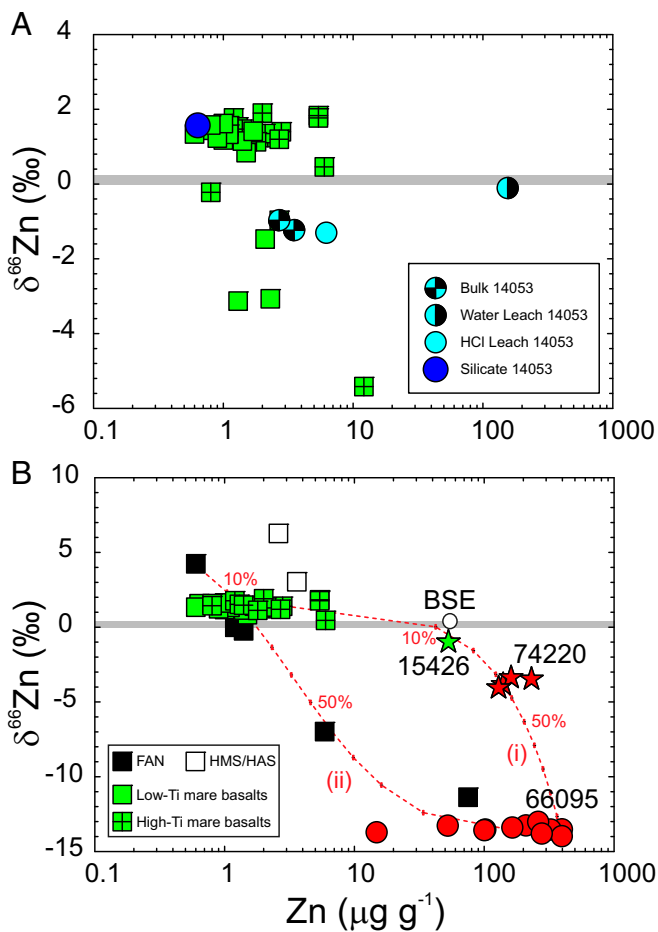


Fig. 3. Zinc concentration versus $\delta^{66}\text{Zn}$ in (A) leaches and residues of Apollo mare basalt 14053 versus published data for low-Ti and high-Ti mare basalts and (B) for 66095, FANs, high-Mg suite and high-alkali suite (HMS/HAS) rocks, lunar volcanic beads (15426, 74220) and mare basalts filtered for condensate Zn addition (values less than chondritic $\delta^{66}\text{Zn}$). Models show simple mixing between average mare basalt and 66095 compositions (i) and 10:1 addition of a sulfidic condensate component to pristine FAN (ii). Gray lines are the terrestrial and chondritic average $\delta^{66}\text{Zn}$ from ref. 3. Data sources are as for Fig. 1, with analytical errors being smaller than symbols.

Dry Versus Damp Moon

The lunar volcanic glass bead samples, 15426 and 74220, were formed by fire fountaining and have high Zn abundances (50 μg·g⁻¹ to 230 μg·g⁻¹) and isotopically light Zn ($\delta^{66}\text{Zn}$ between -1‰ and -4‰) that correlate with bead size (4, 17). The $\delta^{66}\text{Zn}$ values likely reflect condensate Zn on the surfaces of the beads, because the composition of the lunar interior is either expected to be like chondrites and Earth (~+0.3‰), or to have inherited a volatile-depleted signature from the giant impact of >+1.4‰. The volcanic glasses have been shown to have significant enrichments in volatile elements that are surface correlated (30), with lower estimated μ ($^{238}\text{U}/^{204}\text{Pb} = 19$ to 55) than mare basalts [300 to 600 (12, 31)] and high $\delta^{37}\text{Cl}$ [+8.6 to +9.6‰ (6)]. The volcanic glasses also have chondritic relative abundances of the HSE on their outer edges (32), with absolute abundances of these elements that are greater than in mare basalts (33, 34). Collectively, these lines of evidence suggest that the volcanic glass beads have lunar condensate, as well as impactor materials, on their surfaces. The new data for Rusty Rock 66095 indicates that such material was added during fire fountaining, or after the formation of the glass bead deposits. Modeling between a mare basalt source and a 66095 condensate

deposit (Fig. 3) suggests high Zn concentrations on the glass bead surfaces, consistent with observations (4, 17). That 74220 also contains large (>300 μm) olivine grains with melt inclusions containing high OH (up to 1,400 μg·g⁻¹), F, Cl, C, and S contents, and nearly chondritic D/H ratios (13, 14, 35) indicates regions of the Moon's interior may be relatively volatile-rich compared with the source of mare basalts, HMS and alkali-suite rocks, and FANs.

Extreme Zn and Cl isotopic compositions preserved in Rusty Rock 66095 are consistent with derivation from a volatile-poor source within the Moon that experienced progressive outgassing during a lunar magma ocean. Conversely, melt inclusions in a few lunar samples (13, 14) indicate the possibility of volatile-rich sources within the Moon. If the volcanic glasses formed from a primitive melt contaminated by volatile-rich impact materials in the lunar crust (2), and if the olivine also crystallized from this melt, the volatile contents in the glasses would not reflect that of the lunar interior. Instead, interaction with volatile-rich materials would offer a propulsion mechanism for fire fountaining, and explain the presence of condensate Zn in the beads. Such a formation mechanism would also lead to the conclusion of a relatively dry Moon, as indicated by mare basalts, crustal rocks, and even volatile-rich samples, such as the Rusty Rock. Alternatively, if the melt inclusions in the 74220 olivine grains can be shown to have primary magmatic origins, then it is possible that primitive regions of the Moon's interior are relatively volatile-rich compared with the source of mare basalts, HMS and alkali-suite rocks, and FANs.

Materials and Methods

We performed a systematic leaching procedure on three fragments of the Rusty Rock, 66095, 421 (total mass = 163 mg), 66095, 425 (173 mg), and 66095, 430 (201 mg), and 146 mg of a course-grained crush of the mare basalt 14053, 292, measured previously by Kato et al. (4) (SI Appendix and Table S1). The 66095 samples were examined with a binocular microscope, and 66095, 421 and 66095, 430 were found to be dominantly gray crystalline material, with no visible clasts, like fragments of poikilitic impact melt described previously (SI Appendix). Sample 66095, 425 was composed of pale-colored anorthosite-rich material, with black vitrophyric impact melt glass. Imaging of Zn- and Cl-rich phases was done in the same manner as that reported in ref. 23. Leachate and residue samples were measured for trace element abundances, but Re–Os and Rb–Sr isotopes and HSE (Os, Ir, Ru, Pt, Pd, and Re) abundances were only measured in the bulk rocks and residues, due to low quantities (femtograms per gram) of these elements in the leachate.

We used methods for the preparation, purification, and isotopic measurement of Zn that were described previously (24, 36). Zinc purification was achieved using anion-exchange chromatography, with recovery of 99 ± 1%. The blank measured with samples was 5 ng, in line with our previous work (3, 4, 24), and generally represents less than 2% of total measured Zn for most samples (Table S2). Zinc isotopic compositions were measured on a ThermoElectron Neptune Plus multicollector inductively coupled plasma mass spectrometer (MC-ICP-MS) housed at the Institut de Physique du Globe de Paris. Instrumental mass bias was corrected by bracketing each of the samples with standards.

Whole-rock powders, residues, and leachates were measured for bulk-rock trace-element abundances, Sr isotopes, and Re–Os isotope and HSE abundances at the Scripps Isotope Geochemistry Laboratory using established methods (37, 38). Trace-element abundance analyses were done using a ThermoScientific iCAP Qc quadrupole ICP-MS. Trace-element reproducibility of the reference materials was generally better than 5% (relative SD). Strontium isotope measurements were done using a ThermoScientific Triton thermal ionization MS in positive-ion mode; 400-ng loads of National Institute of Standards and Technology Standard Reference Material (NIST SRM) 987 run with the samples gave $^{87}\text{Sr}/^{86}\text{Sr}$ of 0.7102482 ± 48 ($n = 5$), and separate digestions of Basalt, Hawaiian Volcano Observatory (BHVO) 2 prepared with the samples gave $^{87}\text{Sr}/^{86}\text{Sr}$ of 0.7034582 ± 15 ($n = 3$). For Os isotopes and HSE abundances, homogenized powder aliquots of samples were digested in sealed borosilicate Carius tubes, with isotopically enriched multielement spikes (^{99}Ru , ^{106}Pd , ^{183}Re , ^{190}Os , ^{191}Ir , and ^{194}Pt), and 6 mL of a 1:2 mixture of multiply Teflon-distilled HCl and HNO₃ that was purged with H₂O₂ to remove Os. Samples were digested to a maximum temperature of 240 °C in an oven for 72 h. Chemical separation and measurement protocols were identical to those described previously (38). Isotopic compositions of Os were measured in negative-ion mode on a ThermoScientific Triton thermal

ionization MS in negative-ion mode. Rhenium, Pd, Pt, Ru, and Ir were measured using an Cetac Aridus II desolvating nebulizer coupled to the iCAP q ICP-MS. Precision for $^{187}\text{Os}/^{188}\text{Os}$, determined by repeated measurement of the University of Maryland, College Park Johnson–Matthey standard was better than $\pm 0.2\%$ (2 SD; 0.11390 ± 20 ; $n = 5$). External reproducibility on HSE analyses using the iCAP q was better than 0.5% for 0.5 ppb solutions, and all reported values were blank-corrected. Blanks represented between 2% and 6%, 1% and 16%, 0.5% and 6%, 1.5% and 13%, 0.2% and 1.7%, and 0.2% and 2.1% of total measured Re, Pd, Pt, Ru, Ir, and Os, respectively.

Detailed methods and all data associated with this work are archived in the *SI Appendix* accompanying this article.

- Day JMD, Moynier F (2014) Evaporative fractionation of volatile stable isotopes and their bearing on the origin of the Moon. *Philos Trans R Soc London Ser A* 372: 20130259.
- Albarède F, Albalat E, Lee CTA (2015) An intrinsic volatility scale relevant to the Earth and Moon and the status of water in the Moon. *Meteorit Planet Sci* 50:568–577.
- Paniello RC, Day JMD, Moynier F (2012) Zinc isotopic evidence for the origin of the Moon. *Nature* 490:376–379.
- Kato C, Moynier F, Valdes MC, Dhaliwal JK, Day JMD (2015) Extensive volatile loss during formation and differentiation of the Moon. *Nat Commun* 6:7617.
- Wang K, Jacobsen SB (2016) Potassium isotopic evidence for a high-energy giant impact origin of the Moon. *Nature* 538:487–490.
- Sharp ZD, Shearer CK, McKeegan KD, Barnes JD, Wang YQ (2010) The chlorine isotope composition of the moon and implications for an anhydrous mantle. *Science* 329: 1050–1053.
- Boyce JW, et al. (2015) The chlorine isotope fingerprint of the lunar magma ocean. *Sci Adv* 1:e1500380.
- Canup RM (2012) Forming a Moon with an Earth-like composition via a giant impact. *Science* 338:1052–1055.
- Čuk M, Stewart ST (2012) Making the Moon from a fast-spinning Earth: A giant impact followed by resonant despinning. *Science* 338:1047–1052.
- Melosh HJ (1990) Giant impacts and the thermal state of the early Earth. *Origin of the Earth*, eds Newsom H, Jones J (Oxford Univ Press, Oxford), pp 69–83.
- Krahenbuhl U, Ganapathy R, Morgan JW, Anders E (1973) Volatile elements in Apollo 16 samples: Implications for highland volcanism and accretion history of the moon. *Proc Lunar Sci Conf* 4:1325–1348.
- Tatsumoto M, Premo W, Unruh DM (1987) Origin of lead from green glass of Apollo 15426: A search for primitive lunar lead. *J Geophys Res* 92:E361–E371.
- Hauri EH, Weinreich T, Saal AE, Rutherford MC, Van Orman JA (2011) High pre-eruptive water contents preserved in lunar melt inclusions. *Science* 333:213–215.
- Chen Y, et al. (2015) Water, fluorine, and sulfur concentrations in the lunar mantle. *Earth Planet Sci Lett* 427:37–46.
- McCubbin FM, et al. (2015) Magmatic volatiles (H, C, N, F, S, Cl) in the lunar mantle, crust, and regolith: Abundances, distributions, processes, and reservoirs. *Am Mineral* 100:1668–1707.
- Moynier F, Albarède F, Herzog GF (2006) Isotopic composition of zinc, copper, and iron in lunar samples. *Geochim Cosmochim Acta* 70:6103–6117.
- Herzog GF, Moynier F, Albarède F, Berezhnoy AA (2009) Isotopic and elemental abundances of copper and zinc in lunar samples, Zagami, Pele's hairs, and a terrestrial basalt. *Geochim Cosmochim Acta* 73:5884–5904.
- Wanke H, Blum K, Dreibus G, Palme H, Spettel B (1981) Multielement analysis of samples from highlands breccias 66095 (abs). *Proc Lunar Planet Sci Conf* 12: 1136–1138.
- Jovanovic S, Reed GW (1981) Aspects of the history of 66095 based on trace elements in clasts and whole rock. *Proc Lunar Planet Sci Conf* 12:295–304.
- Ebihara M, Wolf R, Warren PH, Anders E (1992) Trace elements in 59 mostly highland moon rocks. *Proc Lunar Planet Sci Conf* 22:417–426.
- Nunes PD, Tatsumoto M (1973) Excess lead in "rusty rock" 66095 and implications for an early lunar differentiation. *Science* 182:916–920.
- Taylor LA, Mao HK, Bell PM (1973) "Rust" in the Apollo 16 rocks. *Proc Lunar Sci Conf* 4:829–839.
- Shearer CK, et al. (2014) Chlorine distribution and its isotopic composition in "rusty rock" 66095. Implications for volatile element enrichments of "rusty rock" and lunar soils, origin of "rusty" alteration, and volatile element behavior on the Moon. *Geochim Cosmochim Acta* 139:411–433.
- Day JMD, Moynier F, Meshik AP, Pradivtseva OV, Petit DR (2017) Evaporative fractionation of zinc during the first nuclear detonation. *Sci Adv* 3:e1602668.
- Day JMD, Brandon AD, Walker RJ (2016) Highly siderophile elements in Earth. *Rev Mineral Geochem* 81:161–238.
- Davis FA, Humayun M, Hirschmann MM, Cooper RS (2013) Experimentally determined mineral/melt partitioning of first-row transition elements (FRTE) during partial melting of peridotite at 3GPa. *Geochim Cosmochim Acta* 104:232–260.
- Beattie P (1993) Uranium–thorium disequilibrium and partitioning on melting of garnet peridotite. *Nature* 363:63–65.
- Snyder GA, Taylor LA, Neal CR (1992) A chemical model for generating the sources of mare basalts: Combined equilibrium and fractional crystallization of the lunar magmasphere. *Geochim Cosmochim Acta* 56:3809–3823.
- Clark RN (2009) Detection of adsorbed water and hydroxyl on the Moon. *Science* 326: 562–564.
- Krahenbühl U (1980) Distribution of volatile and non-volatile elements in grain-size fractions of Apollo 17 drive tube 74001/2. *Proc Lunar Planet Sci Conf* 11:1551–1564.
- Connelly JN, Bizzarro M (2016) Lead isotope evidence for a young formation age of the Earth–Moon system. *Earth Planet Sci Lett* 452:36–43.
- Walker RJ, Horan MF, Schearer CK, Papike JJ (2004) Low abundance of highly siderophile elements in the lunar mantle: Evidence for prolonged late accretion. *Earth Planet Sci Lett* 224:399–413.
- Day JMD, Pearson DG, Taylor LA (2007) Highly siderophile element constraints on accretion and differentiation of the Earth–Moon system. *Science* 315:217–219.
- Day JMD, Walker RJ (2015) Highly siderophile element depletion in the Moon. *Earth Planet Sci Lett* 423:114–124.
- Saal AE, Hauri EH, Van Orman JA, Rutherford MJ (2013) Hydrogen isotopes in lunar volcanic glasses and melt inclusions reveal a carbonaceous chondrite heritage. *Science* 340:1317–1320.
- Moynier F, Le Borgne M (2015) High precision zinc isotopic measurements applied to mouse organs. *J Vis Exp* 99:e52479.
- Day JMD, Peters BJ, Janney PE (2014) Oxygen isotope systematics of South African olivine melilitites and implications for HIMU mantle reservoirs. *Lithos* 202–203:76–84.
- Day JMD, Waters CL, Schaefer BF, Walker RJ, Turner S (2016) Use of hydrofluoric acid desilicification in the determination of highly siderophile element abundances and Re–Pt–Os isotope systematics in mafic-ultramafic rocks. *Geostand Geoanal Res* 40:49–65.